Electrochemical and STM Study of α,ω-alkanedithiols Self-assembled Monolayers

V. C. Ferreira,[a,b] F. Silva,[b] and L. M. Abrantes[a,*]

[a] CQB, Departamento de Química e Bioquímica,
　Faculdade de Ciências da Universidade de Lisboa,
　Campo Grande, 1749-016 Lisboa, Portugal

[b] CIQ-UP, Linha 4, Departamento de Química,
　Faculdade de Ciências da Universidade do Porto,
　Rua do Campo Alegre 687, 4169-007 Porto, Portugal

Self-assembled monolayers (SAMs), prepared by the immersion method, from ethanolic solutions containing α,ω-alkanedithiol, *n*-alkanethiol or mixed thiol/dithiol solutions, with 6, 9 and 10 carbon atoms in the alkyl chain, have been investigated. The amount of adsorbate and the SAM stability in alkaline medium is evaluated by reductive desorption of the prepared monolayers by cyclic voltammetry. An upright orientation of the dithiol self-assembled molecules and disulfide bonding at the SAM/solution interface are suggested by the higher reductive desorption charge of the dithiol monolayers (relative to thiol SAMs) for *n* = 6 and 9. The results show that an improvement on the stability of these dithiol SAMs is obtained by the presence of monothiols, resulting in mixed monolayers. Mixed SAMs prepared from longer alkane chain thiols, *n* = 10, allow to overcome the increased possibility of loop formation and therefore lower surface coverage is obtained for the 1,10-decanedithiol monolayers. Morphological characterisation of the modified electrodes is performed by scanning tunnelling microscopy (STM) *ex situ*, in air. Typical one atom deep thiol induced depressions are observed in the STM images of the dithiol and mixed SAMs.

Key words:
Self-assembled monolayers, α,ω-alkanedithiols, reductive desorption, scanning tunnelling microscopy

Introduction

Self-assembled monolayers (SAMs) of alkanethiols in gold surfaces have been widely studied in the past decades due to their potential applicability in sensors and biosensors development, catalysis and nanoelectronics.[1,2] SAMs of *n*-alkanethiols are the most extensively studied and are commonly used as models in the investigation of other thiol modified surfaces. Although it is still unclear and under active investigation, it is generally accepted that the spontaneous adsorption of thiol molecules on gold (Au) occurs according to Scheme 1, with the formation of a thiolate on the surface.[3,4]

$$R–SH + Au(0) \rightarrow R–S–Au(I) + \tfrac{1}{2}H_2$$
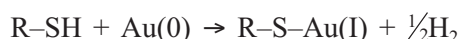
Scheme 1

Alkanethiols are known to form different arrangements depending on the surface crystallographic orientation. In Au(111), scanning tunnelling microscopy (STM) images revealed that *n*-alkanethiols form a hexagonal $(\sqrt{3} \times \sqrt{3})R30°$ structure,[5–10] commensurate with the underlying surface, with a constant periodicity of about 5Å[5,11] and adopt an inclination of ca. 30°,[12–14] relative to the normal with the surface in which the cohesive van der Waals interactions are maximised. Upon thiol adsorption on Au(111), typical depression in the STM images,[5,6,15] filled with highly ordered monolayer,[5,7,8,15] and domains with distinct structural order and size,[6,9,16,17] have been observed. Attempts to elucidate the origins of these depressions in the STM images have passed through the surface reconstruction with compression of the outermost gold layer,[15] dissolution of gold,[8,9,18] and mobility of the Au/thiolate system.[7,18] SAMs have also been electrochemically characterised by cyclic voltammetry (CV), namely by reductive desorption (RD) in alkaline medium. In this case, it has been assumed that one electron is involved per adsorbed molecule according to Scheme 2.[19,20]

$$R–S–Au + 1e^- \rightarrow R–S^- + Au(0)$$
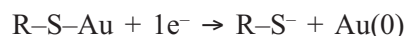
Scheme 2

From the RD cyclic voltammograms it is possible to estimate the amount of adsorbed material, Γ,

through the relation with the charge, Q ($\Gamma = Q/nFA$). In Au(111) a surface coverage of $7.6 \cdot 10^{-10}$ mol cm^{-2} has been found for *n*-alkanethiol SAMs.[10,19,21–25] The RD voltammetric profile of alkanethiol SAMs on gold is also sensitive to the stability of the monolayer, crystallographic orientation and surface crystallinity, alkyl chain length, *n*, and molecular orientation. In fact, it has been reported that for monolayers of alkanethiol on gold, as the cohesive interactions between adsorbed molecules increase with *n*, a potential shift of ca. –20 mV per methylene group occurs;[20,23,26] depending on the surface crystallographic orientation, RD peak potential shifts 200–300 mV between Au(111) and Au(110), translating distinct S–Au bonding energy[27] and the reduction peak can split owing to the presence of dissimilar orientations on the surface.[23,26,27] A peak split with peak potential separation between 20 and 100 mV is also likely to occur due to the existence of molecular domains, with different structural order and size.[25,26]

Due to the strong interaction between sulphur and gold, it is possible to obtain functionalised monolayers through the adsorption of thiols with different functional groups (eg. –OH, –COOH, –NH$_2$ and –SH), allowing to achieve SAMs with distinct chemical and physical properties.[13,28,29]

In the particular case of α,ω-alkanedithiols, the increasing interest devoted to these functionalised SAMs relies on the availability of two thiol functionalities in the molecule (one at each end). The presence of –SH groups, at the SAM/solution interface, enables further surface modification, namely through the interaction with other molecules, ions and particles.[30–35] The α,ω-alkanedithiols self-assembling process and structure is still controversial. Some authors[36–38] used X-ray photoelectron spectroscopy (XPS) to verify that in SAMs prepared with 1,6-hexanedithiol, 1,8-octanedithiol and 1,9-nonanedithiol, from ethanolic solutions, dithiols attach to the surface through a single Au-thiolate bond, similar to alkanethiols, while Leung *et al.*[39] reported that 1,6-hexanedithiol SAMs, prepared from gas phase, adopt a fully extended and parallel to the surface orientation. Experimental and theoretical studies performed by Kohale *et al.*[40] suggest that, for SAMs prepared from solution, the probability of loops formation increases with *n*, being negligible to $n \leq 6$ and starts becoming nonzero for slightly longer dithiols. Intralayer disulfide bonding, due to the availability of –SH groups at the SAM/solution interface, has also been reported,[7,33,38,41] reinforcing the single thiol group attachment to the surface. Interlayer disulfide bonding, resulting in multilayer formation the extent of which depends on the nature of the solvent and presence of oxidising species, has also been suggested.[34,36,38,42,43]

In order to avoid loop formation in the course of dithiol self-assembly, and control the composition, distribution and order of the dithiol SAMs, different approaches have been used, such as co-adsorption of thiol and dithiol molecules[44,45] and insertion of dithiol molecules by exchange reaction.[46,47]

In the present contribution we report the reductive desorption, in alkaline medium, and *ex situ* STM investigation of α,ω-alkanedithiol and mixed thiol/dithiol self-assembled monolayers, prepared from ethanolic solutions. Although dithiol alkyl chain length plays an important role in the stability and organisation of the SAMs, and compact dithiol monolayers were obtained, the presence of alkanethiol molecules, in the preparation solution resulting in mixed monolayers, improved SAMs properties.

Experimental

Pure SAMs were prepared by immersion (22 hours) of the clean gold (111) surface in ethanolic solutions (Panreac, ≥ 99.9 %) containing α,ω-alkanedithiol – C$_n$–SH (1,6-hexanedithiol – C$_6$–SH, 1,9-nonanedithiol – C$_9$–SH and 1,10-decanedithiol – C$_{10}$–SH, AlphaAesar, purity ≥ 95 %) or *n*-alkanethiol – C$_n$ (1-hexanethiol – C$_6$, 1-nonanethiol – C$_9$ and 1-decanethiol – C$_{10}$, AlphaAesar, purity ≥ 96 %). Mixed SAMs were obtained from solutions containing both thiol and dithiol molecules, with equal chain length, n = 6, 9 and 10 (22 hours). The pure α,ω-alkanedithiol and *n*-alkanethiol SAMs will be referred to as dithiol and thiol SAMs, respectively, and mixed SAMs as m-C$_n$ SAM, where *n* indicates the alkyl chain length.

Gold-coated slides (1.1 · 1.1 cm^2, Gold Arrandee, Germany) were used; the surfaces were cleaned with *piranha* solution, rinsed with copious amounts of ultrapure water and ethanol, and flame annealed, leading to a predominantly (111) crystallographic orientation and a surface roughness R = 1.2.

Electrochemical experiments were performed with an IMT Electrochemical Interface and a DEA332 Digital Electrochemical Analyser connected to a computer for data acquisition (VoltaMaster2 software). A one-compartment cell was used, with the gold-coated glass as working electrode (0.57 cm^2 exposed geometrical area), a Pt wire counter-electrode and a saturated calomel reference electrode (SCE).

Following SAMs preparation, the gold slides were removed from the solution, rinsed with ethanol and water, and transferred to the electrochemical cell. The SAMs were electrochemically characterised by reductive desorption (by means of poten-

tial cycling at $\nu = 20$ mV s^{-1} between 0 and -1.20 or -1.25 V) in 0.1 mol dm^{-3} NaOH solution (Panreac, p.a.). The sample-to-sample variability in the peaks position is ± 10 mV.

Prior to all measurements, the solutions, prepared with Milli-Q water, were degassed with N$_2$ (99.9999 %) for 1 hour.

The morphological characterisation of SAMs was performed by scanning tunneling microscopy (STM) *ex situ*, in a Multimode – Nanoscope IIIa (Digital Instruments) and mechanically cut Pt-Ir tips were used. Average tunneling current of 150 pA and ca. 800 mV bias were employed throughout the experiments.

Results and discussion

α,ω-Alkanedithiol self-assembled monolayers

Reductive desorption

Figs. 1 and 2 illustrate the cyclic voltammograms obtained for the reductive desorption of α,ω-alkanedithiol and *n*-alkanethiol pure SAMs, respectively, with different alkyl chain length ($n = 6$, 9 and 10), in NaOH 0.1 mol dm^{-3} solution. In general, two reduction peaks are observed in the cathodic scan and a single oxidation peak in the anodic scan. The last has been attributed to the re-adsorption of the desorbed products.[21,22] The presence of two reduction peaks in the voltammetric profiles has been assigned either to the presence of molecular domains within the monolayer[25,26] or to the microscopic surface roughness,[23,26,27] with different binding strengths at dissimilar type of binding sites. The peaks (1 and 2) potential separation, ΔE^c, is about 149 mV and 65–120 mV, for the dithiol and thiol SAMs respectively. Contributions from both

F i g . 2 – *Cyclic voltammograms of the reductive desorption of (——) 1-hexanethiol, (– – –) 1-nonanethiol and (·····) 1-decanethiol SAMs; NaOH 0.1 mol dm^{-3}, $\nu = 20$ mV s^{-1}*

factors can be considered, given that peak potential shifts of 200–300 mV, translating distinct S–Au bonding energy[27] and reduction peak split, due to the presence of dissimilar orientations on the surface[23,26,27] and molecular domains in the monolayer with peak separation between 20–100 mV,[25,26] have been reported for *n*-alkanethiol SAMs.

Table 1 summarises the peaks potential values, reduction peaks separation and surface coverage, Γ, obtained from Fig. 1 and 2. Γ values were estimated from the charge under the reduction peaks, assuming one electron per adsorbed molecule.[10,19–25]

As expected, the stability of the α,ω-alkanedithiol SAMs slightly increases with the alkyl chain length of the adsorbed molecules (the reductive desorption peak 1, E_1^c, is shifted to more negative values), which is due to the van der Waals interaction between alkyl chains. In the case of *n*-alkanethiol SAMs, the peak potential shift with *n*, is larger than that for the dithiol SAMs, suggesting that the presence of the second thiol group decreases the van der Waals interactions.

The reductive desorption of the SAMs prepared from 1,6-hexanedithiol using 8 h immersion time occurs at less negative potential values than those formed for longer periods (22 h), revealing its lower stability; in spite of this, the surface coverage of both monolayers are similar, indicating that the SAM organisation is much slower than the thiol adsorption step, as it has been reported in the literature.[7,29,41]

As depicted in Table 1, the reductive desorption features (reduction peaks potential and surface coverage values) do not change significantly with the scan rate, suggesting that at $\nu = 20$ mV s^{-1} the SAM desorption is also completed. However, for the 1,10-decanedithiol SAM,
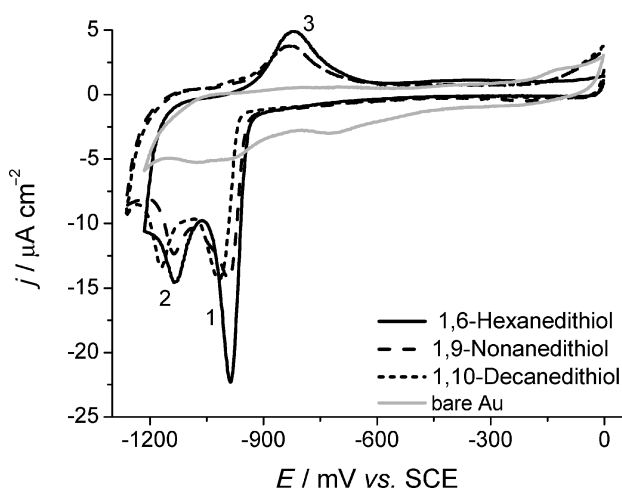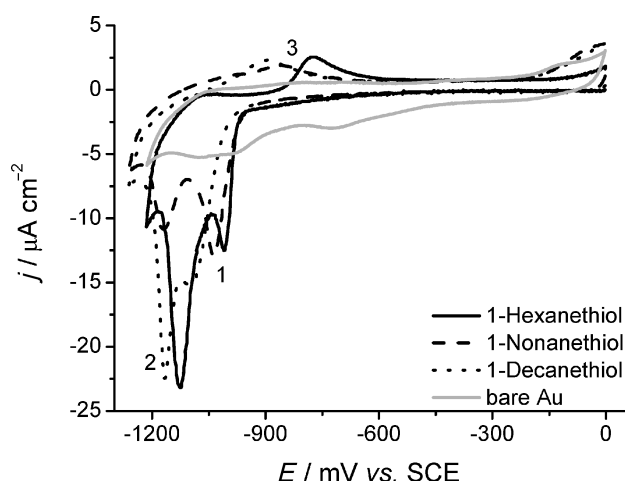

F i g . 1 – *Cyclic voltammograms of the reductive desorption of (——) 1,6-hexanedithiol, (– – –) 1,9-nonanedithiol and (·····) 1,10-decanedithiol SAMs; NaOH 0.1 mol dm^{-3}, $\nu = 20$ mV s^{-1}*

T a b l e 1 – *Values of reductive desorption and re-oxidation peaks potential and surface coverage, Γ, for the α,ω-alkanedithiols and n-alkanethiol SAMs*

Thiol	t/h	ν/mV s^{-1}	E^c/mV		E^a_3/mV	$\Delta E^c_{(2-1)}$/mV	$10^{10}\ \Gamma\ (\pm 0.32)$/mol cm^{-2}
			1	2			
1-hexanethiol	22	20	−1008	−1126	−774	118	6.55
1,6-hexanedithiol	8	10	−942	−1024	−837	82	7.42
	22	20	−988	−1135	−821	147	7.30
1-nonanethiol	22	20	−1041	−1161	−860	120	5.46
1,9-nonanedithiol			−992	−1138	−832	146	6.30
1-decanethiol	22	20	−1100	−1165	−897	65	7.39
1,10-decanedithiol		10	−1016	−1179	−845	163	6.12
		20	−1018	−1170	−828	152	6.22

E – Cathodic (c) and anodic (a) peaks potential values; ΔE^c – cathodic peaks separation; Γ – surface coverage

Fig. 3a, the charge involved in the reductive desorption peak (cycle 2) is not fully explainable by the oxidative re-deposition, i.e. the oxidation peak 3 (cycle 1); this trend is much less pronounced for the thiol SAMs, Fig. 3b. The observed behaviour is very likely due to the availability of the second thiol functionality for a spontaneous re-adsorption, occurring with zero current flow.[48]

The obtained surface coverage values for both dithiol and thiol SAMs are in agreement with those reported in the literature for compact *n*-alkanethiol monolayers, $\Gamma = 7.6 \cdot 10^{-10}$ mol cm^{-2},[10,19,21–25] thus pointing to the formation of well packed dithiol monolayers. It is noteworthy that for the shorter chain length dithiol SAMs (n = 6 and 9), the Γ values are higher than those obtained for the corresponding thiol SAMs. The availability of –SH groups at the SAM/solution interface, enabling the disulfide bonds formation at this interface, may contribute to the cathodic charge and therefore to the estimated Γ values; similar behaviour has already been reported.[33,41] For the 1,10-decanedithiol SAMs, the probability of loop formation,[40] must be taken into account since it induces disorder on the monolayer leading to the observed lower Γ values when compared with the 1-decanethiol SAM.

Scanning tunnelling microscopy characterisation

In Fig. 4 are illustrated the STM images obtained for the pure SAMs prepared from *n*-alkanethiols and α,ω-alkanedithiols. The presence of the thiol and dithiol monolayers in the gold surface is evident from the typical one atom deep depressions, induced by the thiol, in the large gold ter-
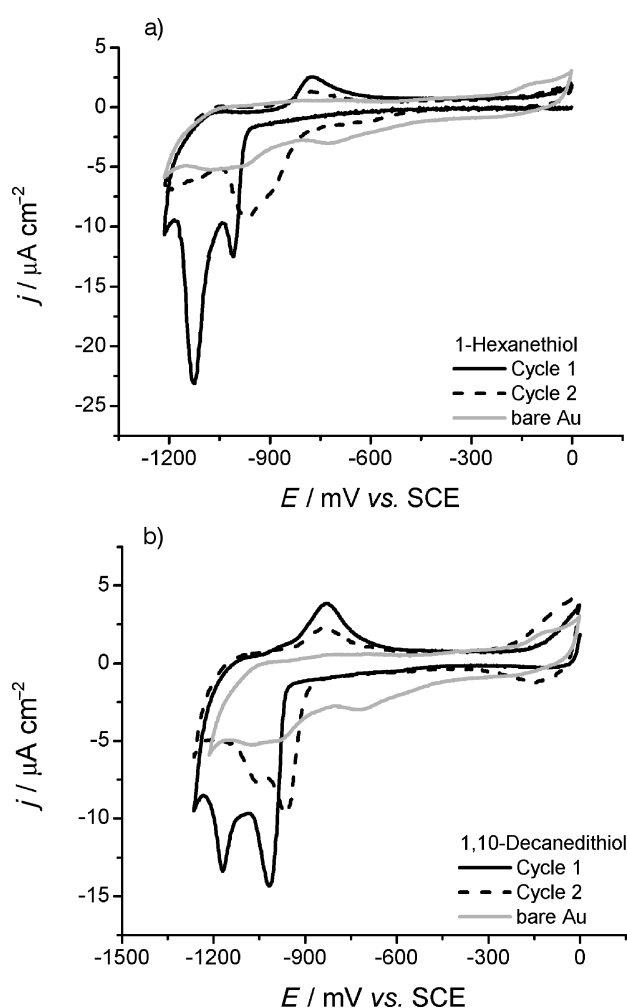

F i g . 3 – *Cyclic voltammograms of the reductive desorption of (a) 1,10-decanedithiol and (b) 1-hexanethiol SAMs, (——) first cycle and (– – –) second cycle; NaOH 0.1 mol dm^{-3}, ν = 20 mV s^{-1}*
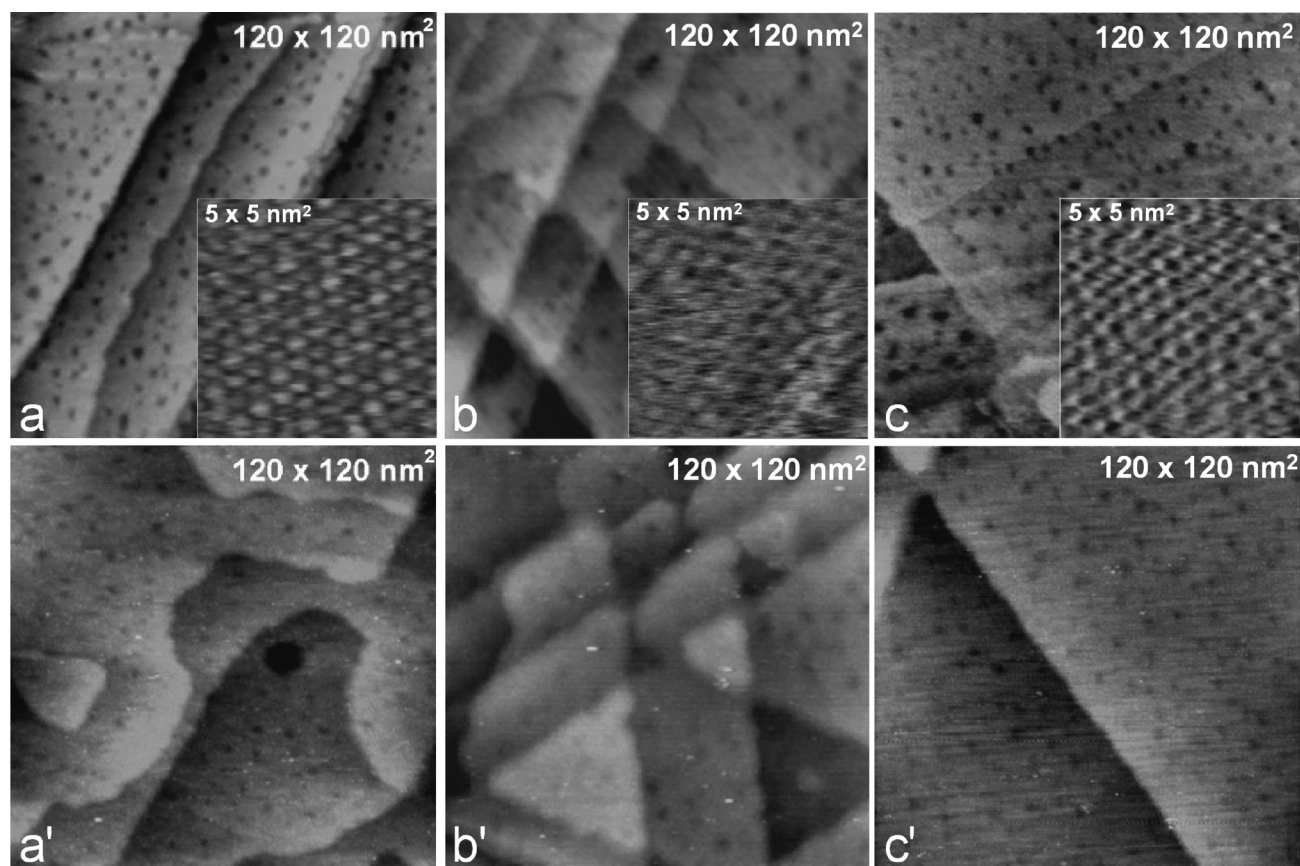
F i g . 4 – *STM images of the SAMs prepared from ethanolic solutions of n-alkanethiols: (a) 1-hexanethiol (z = 4 nm), (b) 1-nonanethiol (z = 2 nm) and (c) 1-decanethiol (z = 2 nm) (inset: n-alkanethiols 5 × 5 nm² images) and α,ω-alkanedithiols: (a') 1,6-hexanedithiol (z = 2 nm), (b') 1,9-nonanedithiol (z = 2 nm) and (c') 1,10-decanedithiol (z = 1 nm); 120 × 120 nm² images, $i_T \approx$ 150 pA and $U_T \approx 800$ mV*

races. For the SAMs prepared from *n*-alkanethiols, presented in Fig. 4 a–c, a hexagonal structure, commensurate with the underlying (111) gold surface, was detected in a small scan area (5×5 nm², insets of Fig. 4 a–c).

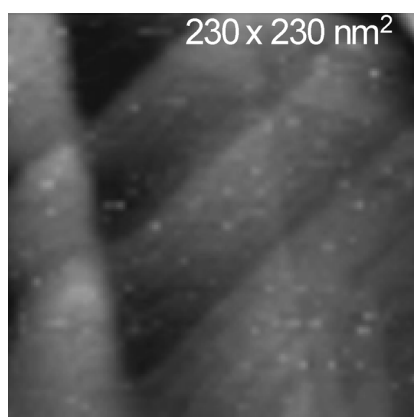The lack of molecular resolution in the STM images of the α,ω-alkanedithiols SAMs (Fig. 4

F i g . 5 – *STM image of the SAM prepared from ethanolic solutions of 1,9-nonanedithiol (z = 6 nm); 230 × 230 nm² images, $i_T \approx 500$ pA and $U_T \approx 200$ mV*

a'–c') corroborates the low organisation of the dithiol monolayers, suggested by the electrochemical data. In this case, clusters with less than 1 nm height can be detected in the STM images which are not observable in the alkanethiol monolayers images, Fig. 5.

As far as we know, the nature of these clusters has not been discussed in the literature but one possible cause for its presence may be the formation of more than one monolayer due to the formation of disulfide bonds with free molecules from the solution.

Mixed self-assembled monolayers

Reductive desorption

The insertion of alkanethiol molecules in dithiol monolayers has been successfully used to decrease alkanedithiol looping and to enhance the stability and organisation of the SAMs prepared from dithiols, enabling the availability of –SH groups at the SAM/solution interface as well as to produce nanopatterned SAMs.[44,45,47] A simple and convenient approach to achieve mixed SAMs is the

employment of assembling solutions containing both thiol and dithiol molecules;[44,45] it is known that different parameters, such as thiol to dithiol ratio, thiols/dithiols solubility and chain length, influence the distribution and amount of each component in the monolayer.[44,45,49,50]

Fig. 6 contrasts the electrochemical characterisation of the mixed SAMs, m-C$_n$, prepared from ethanolic solutions containing thiol and dithiol molecules with the same chain length (n = 6, 9 or 10), with the corresponding dithiol and thiol monolayers.

As can be seen in Table 2, the increase of the *n*-alkanethiol concentration in the preparation solution (thiol to dithiol ratio from (1:1) to (3:1)) enhances the surface coverage, suggesting that the monothiol induces the organisation and stabilisation of the monolayer. This is also corroborated by the potential shift of the cathodic peaks to more negative values in mixed SAMs (n = 6 and 9) when compared with dithiol monolayers, as shown in the Fig. 6a and b.

For the longest alkyl chain length (cyclic voltammograms displayed in Fig. 6c) the cathodic peak occurs at about the same potential values for dithiol and mixed SAMs; the presence of the alkanethiol in this mixed SAM seems to hinder the loop formation and an increase in the surface coverage is achieved (Table 2). Since the anodic peak potential values agree with those observed for the corresponding dithiol SAMs, dithiol can be assumed as the main component of the mixed SAMs.

Scanning tunnelling microscopy characterisation

In the case of dithiol molecules inserted in the alkanethiol monolayers[47] and in mixed SAMs of aromatic dithiols and 1-octanethiol,[45] it has been possible to reach molecular resolution in the STM images, for *as prepared* SAMs. However, besides some phase segregation, it appears very difficult to observe structural features in less organised mixed SAMs[51,52] and simple dithiol monolayers.[7,39,41]
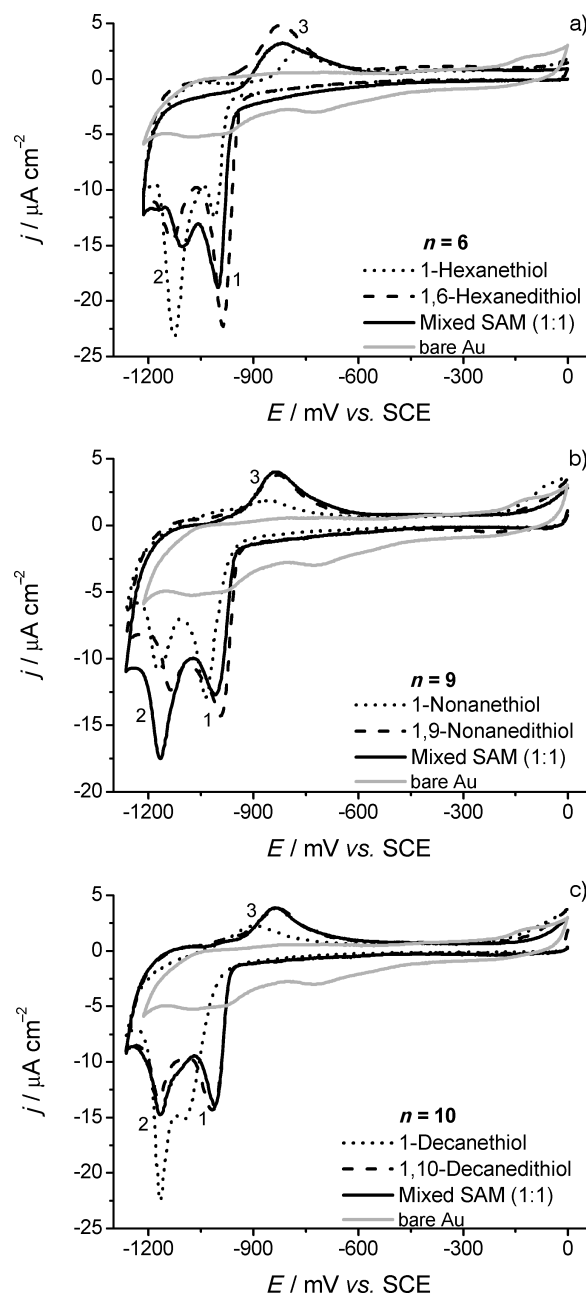

F i g . 6 – *Cyclic voltammograms of the reductive desorption of the mixed SAMs prepared from ethanolic solutions containing: (a) 1,6-hexanedithiol/1-hexanethiol, (b) 1,9-nonanedithiol/1-nonanethiol and (c) 1,10-decanedithiol/1-decanethiol and comparison with pure (·········) n-alkanethiol and (– – –) α,ω-alkanedithiol SAMs with equal chain length; NaOH 0.1 mol dm^{-3}, v = 20 mV s^{-1}*

T a b l e 2 – *Values of reductive desorption and re-oxidation peaks potential and surface coverage, Γ, for the mixed SAMs*

Thiol/Dithiol		t/h	v/mV s^{-1}	E^c/mV		E^a_3/mV	$\Delta E^c_{(2-1)}$/mV	10^{10} Γ ($\pm$ 0.20)/mol cm^{-2}
				1	2			
C$_6$/C$_6$–SH	(1:1)	22	20	−1003	−1104	−817	101	5.15
	(3:1)			−1028	−1087	−808	59	5.85
C$_9$/C$_9$–SH	(1:1)	22	20	−1010	−1166	−837	156	6.16
C$_{10}$/C$_{10}$–SH	(1:1)	22	20	−1012	−1165	−839	153	6.62

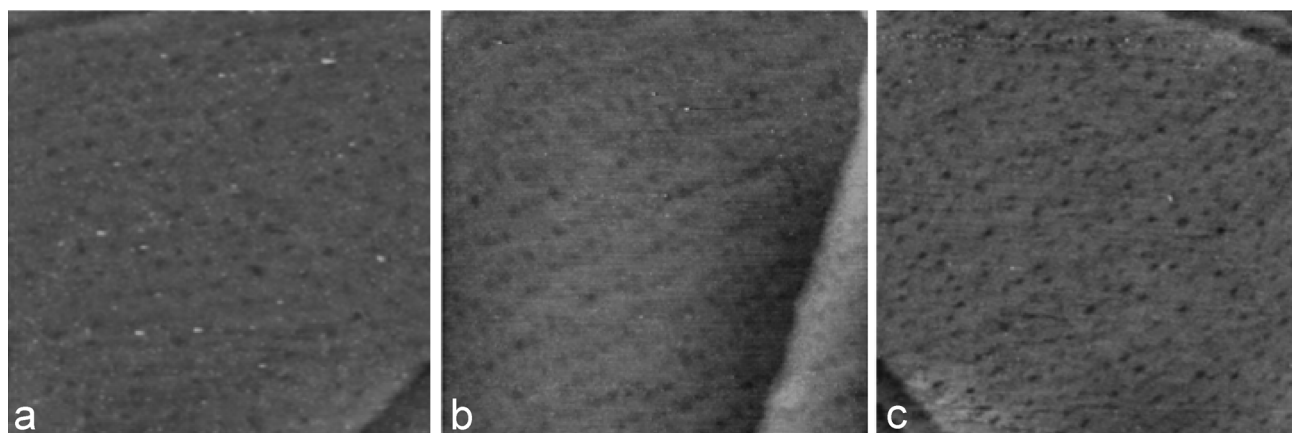*E* – Cathodic (c) and anodic (a) peaks potential values; Δ*E*^{c} – cathodic peaks separation; *Γ* – surface coverage

F i g . 7 – *STM images of the mixed SAMs prepared from: (a) 1-hexanethiol/1,6-hexanedithiol (z = 2 nm), (b) 1-nonanethiol/1,9-no-nanedithiol (z = 1 nm) and (c) 1-decanethiol/1,10-decanedithiol (z = 1 nm), (1:1) ethanolic solutions; 120 × 120 nm^2 images, $i_T \approx 150$ pA and $U_T \approx 800$ mV*

Fig. 7 illustrates the STM images obtained for the mixed SAMs (with the typical depressions confirming its formation).

In spite of the improved stability and loop formation decrease indicated by the electrochemical data, it was not possible to achieve molecular resolution in the STM images of m-C_n SAMs. This is related probably to the SAMs composition, with the dithiol as the major component.

Conclusions

The stability and organisation of the dithiol SAMs in Au(111) are dependent on the adsorption time and alkyl chain length, although to a lower extent than observed for the *n*-alkanethiol SAMs. The presence of molecular domains and some surface roughness was suggested by the occurrence of two reduction peaks in the cyclic voltammograms.

The second thiol functionality in the dithiol molecules induces disorder in the SAMs, as evidenced by the reduction peaks potential shift to less negative values than observed for alkanethiol SAMs and by the lack of molecular resolution in the STM images. Nevertheless, the formation of the SAMs on the Au(111) surface has been confirmed by the presence of typical one atom deep depressions on the STM images.

α,ω-Alkanedithiols in Au(111) seem to adopt an upright orientation of the dithiol molecules self-assembled on Au, with adsorption through a single –SH group and formation of disulfide bonds at the SAM/solution interface which was corroborated by the higher reduction charge of dithiol monolayers (*n* = 6 and 9), than for *n*-alkanethiol SAMs. Long alkyl chain dithiols (*n* = 10) showed a greater tendency toward loop formation and surface coverage decreases.

Mixed SAMs displayed higher stability and organisation than α,ω-alkanedithiols monolayers. Increasing concentration of *n*-alkanethiol in the preparation solution enhances surface coverage and decreases loop formation for longer alkyl chain dithiols.

List of Symbols

E – cathodic (c) and anodic (a) potential
ΔE – potential difference
ν – scan rate
Γ – surface coverage
Q – charge
n – number of electrons
A – area
R – surface roughness
i_T – tunnelling current
U_T – bias

References

1. *Mirsky, V.,* Trends Anal. Chem. **21** (2002) 439.
2. *Love, J. C., Estroff, L. A., Kriebel, J. K., Nuzzo, R. G., Whitesides, G. M.,* Chem. Rev. **105** (2005) 1103.
3. *Schlenoff, J. B., Li, M., Ly, H.,* J. Am. Chem. Soc. **117** (1995) 12528.
4. *Ulman, A.,* Chem. Rev. **96** (1996) 1533.

5. *Schonenberger, C., Jorritsma, J., Sondag-Huethorst, J. A. M., Fokkink, L. G. J.,* J. Phys. Chem. **99** (1995) 3259.

6. *Delamarche, E., Michel, B., Kang, H., Gerber, C.,* Langmuir **10** (1994) 4103.

7. *Esplandiu, M. J., Carot, M. L., Cometto, F. P., Macagno, V. A., Patrito, E. M.,* Surf. Sci. **600** (2006) 155.

8. *Schonenberger, C., Sondag-Huethoorst, J. A. M., Jorritsma, J., Fokkink, L. G. J.,* Langmuir **10** (1994) 611.

9. *Poirier, G. E., Tarlov, M. J.,* Langmuir **10** (1994) 2853.

10. *Widrig, C. A., Alves, C. A., Porter, M. D.,* J. Am. Chem. Soc. **113** (1991) 2805.

11. *Chidsey, C. E. D., Liu, G.-Y., Rowntree, P., Scoles, G.,* J. Chem. Phys. **91** (1989) 4421.

12. *Porter, M. D., Bright, T. B., Allara, D. L., Chidsey, C. E. D.,* J. Am. Chem. Soc. **109** (1987) 3559.

13. *Nuzzo, R. G., Dubois, L. H., Allara, D. L.,* J. Am. Chem. Soc. **112** (1990) 558.

14. *Mar, W., Klein, M. L.,* Langmuir **10** (1994) 188.

15. *McDermott, C. A., McDermott, M. T., Green, J.-B., Porter, M. D.,* J. Phys. Chem. **99** (1995) 13257.

16. *Camillone III, N., Chidsey, C. E. D., Liu, G.-Y., Scoles, G.,* J. Chem. Phys. **98** (1993) 4234.

17. *Duwez, A.-S., Yu, L. M., Ruga, J., Pireaux, J.-J., Delhalle, J.,* Thin Solid Films **327-329** (1998) 156.

18. *McCarley, R. L., Kim, Y.-T., Bard, A. J.,* J. Phys. Chem. **97** (1993) 211.

19. *Walczak, M. M., Popenoe, D. D., Deinhammer, R. S., Lamp, B. D., Chung, C., Porter, M. D.,* Langmuir **7** (1991) 2687.

20. *Widrig, C. A., Chung, C., Porter, M. D.,* J. Electroanal. Chem. **310** (1991) 335.

21. *Yang, D.-F., Wilde, C. P., Morin, M.,* Langmuir **13** (1997) 243.

22. *Yang, D.-F., Wilde, C. P., Morin, M.,* Langmuir **12** (1996) 6570.

23. *Walczak, M. M., Alves, C. A., Lamp, B. D., Porter, M. D.,* J. Electroanal. Chem. **396** (1995) 103.

24. *Strong, L., Whitesides, G. M.,* Langmuir **4** (1988) 546.

25. *Wong, S.-S., Porter, M. D.,* J. Electroanal. Chem. **485** (2000) 135.

26. *Zhong, C.-J., Porter, M. D.,* J. Electroanal. Chem. **425** (1997) 147.

27. *Zhong, C.-J., Zak, J., Porter, M. D.,* J. Electroanal. Chem. **421** (1997) 9.

28. *Chidsey, C. E. D., Loiacono, D. N.,* Langmuir **6** (1990) 682.

29. *Bain, C. D., Troughton, E. B., Tao, Y.-T., Evall, J., Whitesides, G. M., Nuzzo, R. G.,* J. Am. Chem. Soc. **111** (1989) 321.

30. *Nakanishi, T., Ohtani, B., Uosaki, K.,* J. Phys. Chem. B **102** (1998) 1571.

31. *Brust, M., Blass, P. M., Bard, A. J.,* Langmuir **13** (1997) 5602.

32. *Deng, W., Yang, L., Fujita, D., Nejoh, H., Bai, C.,* Appl. Phys. A **71** (2000) 639.

33. *Esplandiu, M. J., Hagenstrom, H.,* Solid State Ionics **150** (2002) 39.

34. *Liang, J., Rosa, L. G., Scoles, G.,* J. Phys. Chem. C **111** (2007) 17275.

35. *Ohgi, T., Sheng, H.-Y., Nejoh, H.,* Appl. Surf. Sci. **130-123** (1998) 919.

36. *Rieley, H., Kendall, G. K., Zemicael, F. W., Smith, T. L., Yang, S.,* Langmuir **14** (1998) 5147.

37. *Esplandiu, M. J., Noeske, P.-L. M.,* Appl. Surf. Sci. **199** (2002) 166.

38. *Kohli, P., Taylor, K. K., Harris, J. J., Blanchard, G. J.,* J. Am. Chem. Soc. **120** (1998) 11962.

39. *Leung, T. Y. B., Gerstenberg, M. C., Lavrich, D. J., Scoles, G.,* Langmuir **16** (2000) 549.

40. *Kohale, S., Molina, S. M., Weeks, B. L., Khare, R., Hope-Weeks, L. J.,* Langmuir **23** (2007) 1258.

41. *Carot, M. L., Esplandiu, M. J., Cometto, F. P., Patrito, E. M., Macagno, V. A.,* J. Electroanal. Chem. **579** (2005) 13.

42. *Joo, S. W., Han, S. W., Kim, K.,* Langmuir **16** (2000) 5391.

43. *Joo, S. W., Han, S. W., Kim, K.,* J. Phys. Chem. B **104** (2000) 6218.

44. *Alianga, A. K. A., Duwez, A.-S., Mittler, S.,* Org. Electron. **7** (2006) 337.

45. *Jiang, W., Zhitenev, N., Bao, Z., Meng, H., Abusch-Magder, D., Tennant, D., Garfunkel, E.,* Langmuir **21** (2005) 8751.

46. *Meshulam, G., Rosenberg, N., Caster, A., Burstein, L., Gozin, M., Richter, S.,* Small **1** (2005) 848.

47. *Fuchs, D. J., Weiss, P. S.,* Nanotechnology **18** (2007) 044021.

48. *Schneider, T. W., Buttry, D. A.,* J. Am. Chem. Soc. **115** (1993) 12391.

49. *Laibinis, P. E., Fox, M. A., Folkers, J. P., Whitesides, G. M.,* Langmuir **7** (1991) 3167.

50. *Folkers, J. P., Laibinis, P. E., Whitesides, G. M.,* J. Phys. Chem. **98** (1994) 563.

51. *Stranick, S. J., Atre, S. V., Parikh, A. N., Wood, M. C., Allara, D. L., Winograd, N., Weiss, P. S.,* Nanotechnology **7** (1996) 438.

52. *Phong, P. H., Sokolov, V. V., Nishi, N., Yamamoto, M., Kakiuchi, T.,* J. Electroanal. Chem. **600** (2007) 35.